1 Introduction

Since the first passenger car with an internal combustion (IC) engine was developed over 120 years ago, the device has been significantly improved regarding efficiency, emissions, smoothness and ease of use. Today IC-engines are used in roughly 850 million passenger cars worldwide. Even though many other concepts such as fuel cells are investigated, it seems that no system can replace IC-engines in the near and intermediate future.

Two different combustion concepts are considered to have the potential to fulfill future requirements with respect to fuel consumption and emission standards: turbo-charged diesel and stratified spark ignition (SI) engines with high pressure direct injection (DI) systems. Both systems can operate with overall lean air/fuel mixtures.

The first DISI-engine in a passenger car used a homogeneous air/fuel mixture. It was implemented in 1951 in the models Gutbrod Superior and Goliath GP 700 leading to a significant reduction in fuel consumption. The first application in mass production of direct injection systems in SI-engines was in 1997 in the Mitsubishi Carisma GDI (gasoline direct injection).

The greatest challenges facing stratified DISI-engines today, which give a much higher potential in fuel consumption economy compared to the homogeneous combustion concept, are combustion stability and emissions. Cycle-to-cycle variations of the gas motion have been identified to play a key role in the further optimization of the device since they have a great impact on the combustion process. Engine parameters are set according to the behavior of the mean cycle. However, the extreme engine cycles, cycles of greatest and slowest burning rates, determine the operating range of the engine. Consequently, the optimal spark timing, equivalence ratio and compression ratio are compromised. A critical issue in stratified DISI-engines is that cyclic variations are substantial to the combustibility of the air/fuel mixture at the time of the discharge of the spark plug leading to partial burning or even misfire. This phenomenon is undesirable in terms of engine roughness, efficiency and unburned hydrocarbon emissions.

Computational fluid dynamics (CFD) with common Reynolds averaged Naviers-Stokes (RANS) turbulence modeling has been established to be a very efficient and reliable tool within the design process of IC-engines. Optimization of engine geometries can be accomplished with a short turnaround time. Additionally, insights into various physical processes can be gained that are difficult to study experimentally. However, this approach is limited by definition if unsteady features such as cycle-to-cycle variations are investigated and cannot capture this kind of phenomenon.

On the other hand, large eddy simulation (LES) provides the ability to predict cyclic variations because smaller spatial scales and temporal fluctuations are resolved. Since in LES a significantly smaller range of turbulent length scales needs to be modeled compared to the RANS approach, the accuracy of LES is superior to RANS. However, resolving smaller temporal and spatial scales requires higher order numerical schemes, smaller time steps and

higher resolutions of the computational grids. This can lead to a significant increase of CPU-time compared to RANS.

For wall-bounded turbulent flows at high Reynolds number and in complex geometries hybrid RANS/LES approaches have become more and more popular in the recent years. They combine attractive features of both methods. These methods provide the opportunity to use LES in regions, where its performance is known to be essentially superior to RANS. In other regions where the accuracy and the averaged information on turbulent properties is sufficient RANS can be used in order to save CPU-time. In contrast to pure RANS, temporal fluctuations can be resolved in the LES regions in hybrid methods giving these approaches the potential to predict cycle-to-cycle variations or other turbulent flows of highly unsteady nature.

The present work focuses on unsteady turbulent flow phenomena in IC-engines such as cyclic variations of the gas motion and investigates the ability of subgrid turbulence modeling to predict them. In Chapter 2 the basic physical principles of fluid dynamics and turbulent flows are described both phenomenologically and based on the underlying governing equations. Furthermore, a review of filtering operations applied to the Navier Stokes equations and state of the art turbulence modeling is given. The different methods as well as the corresponding specific treatment of the boundary conditions of conventional RANS simulation and LES are presented and the hybrid RANS/LES method is introduced.

The numerical requirements for the hybrid approach in terms of spatial and temporal schemes as well as the meshing method that is needed for the computation of flows in complex geometries with moving boundaries as in IC-engines are described in Chapter 3. Different numerical schemes of the CFD code CFX, which are used in this work, are evaluated and tested against the numerics of other commercial and academic codes.

In Chapter 4 the hybrid method is tested against measurements and data of direct numerical simulation (DNS) for simple flow cases. For a fundamental evaluation of the approach classic turbulence test cases such as the decay of homogeneous isotropic turbulence and the flow past a backward-facing step are used. The most relevant flow configurations in engine development are the steady flow through an intake port/valve assembly and the transient flow in a reciprocating engine. However, before the hybrid method is applied to these complex turbulent flows in IC-engines at high Reynolds number, simplified configurations of theses cases are investigated. The hybrid RANS/LES method is compared to RANS and LES computations in terms of accuracy and level of information of turbulence properties.

Chapter 5 is dedicated to flows in IC-engines. The specific flow characteristics are described and quantified and key issues in engine design are discussed. The hybrid RANS/LES method is used for the computation of the steady flow through an intake port and the multi-cycle simulation of the flow in a series production BMW engine. Optical measurements are used to evaluate the quality of the averaged flow field of the simulation as well as the ability to predict cyclic variations of the gas motion in IC-engines.

2 Theory

2.1 Phenomenological Description of Turbulence

Prior to the detailed description of the governing equations and appropriate modeling approaches basic concepts of turbulence are presented.

A turbulent flow field is characterized by quasi-random, time-dependent, three-dimensional variations of all properties in fluid mechanics over a large range of time and length scales. The common global quantity, which is used to classify turbulence, is the Reynolds number $Re = \frac{\mathscr{U}\mathscr{L}}{\nu}$. $\mathscr{L}$ and $\mathscr{U}$ are the characteristic length scale and characteristic velocity of the flow, respectively, and ν denotes the kinematic molecular viscosity of the fluid. In turbulent flows with high Reynolds numbers there exists a complete hierarchy of time and length scales. In order to analyze these scales and to investigate the nature of turbulence, the phenomena is investigated using several methods such as spectral and statistical analysis and the anisotorpy-invariant theory. The following discussion is for incompressible flows.

2.1.1 The Energy Spectrum

Fig. 2.1 shows the three-dimensional *energy spectrum* for homogeneous isotropic turbulence based on the Kármán-Pao model spectrum, which will be discussed in further detail in section 3.1.2.

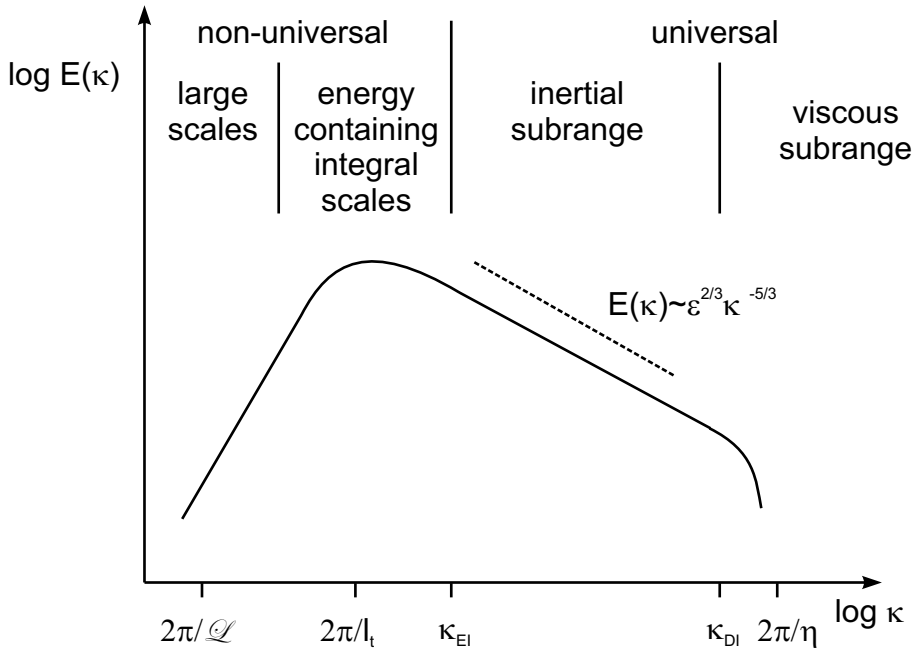

Figure 2.1: Sketch of a Kármán-Pao energy spectrum for homogeneous isotropic turbulence.

An energy spectrum $E(\kappa)$ can be extracted from the turbulent velocity field by spatial Fourier-transformation. $E(\kappa)$ is the energy contained in the eddies of a certain size l expressed by the

corresponding wavenumber $\kappa = 2\pi/l$. The energy, which is contained in all eddies over the full range of turbulent length scales, is the turbulent kinetic energy k. It is obtained by the integral over all turbulent wavenumbers and corresponds to the area under the energy cascade in **Fig. 2.1**:

$$k = \int_0^\infty E(\kappa) d\kappa \quad . \tag{2.1}$$

The scales of the energy spectrum can be divided into several subranges. The large spatial scales of turbulent motion are determined by the geometry of the domain and the boundary conditions and are not universal for that reason. The size of the most energetic eddies is of the order of the turbulent length scale l_t. Anisotropy is confined to these scales and also turbulent kinetic energy is produced by the mean velocity gradients in this range. According to the theory of the *energy cascade* for high Reynolds number flows introduced by Richardson (1922) and refined by Kolmogorov (1941), there is a continuous break down process and inviscid energy transfer in the inertial subrange to successively smaller eddies. The process continues until the smallest eddies of the size of the Kolmogorov length scale η dissipate due to the dominance of viscous forces in the viscous subrange. Limited in time and space there is also an energy transfer from the smaller to the larger turbulent structures, which is referred to as the *backscatter-effect*. It has been estimated that roughly a third of the energy that is transferred from the large to the small scales flows back in the opposite direction. The rate of the energy conversion of the kinetic energy of the smallest eddies into thermal energy is referred to as turbulent or eddy dissipation rate ε. It can be expressed in relation to $E(\kappa)$ as follows:

$$\varepsilon = \int_0^\infty 2\nu\kappa^2 E(\kappa) d\kappa \quad . \tag{2.2}$$

There is no turbulent production in the inertial subrange and the energy transfer is local in the sense that the energy of an eddy of a certain length scale is only transferred to the next smaller eddy. Due to the locality of the energy transfer and the absence of production of energy, the rate of the energy transfer in the cascade equals the turbulent dissipation rate ε. This rate is constant and scale-invariant in the inertial subrange. The scale invariance is one of the most important assumptions in turbulence modeling and has been applied in a variety of models. According to the *second similarity hypothesis of Kolmogorov* for sufficiently high Reynolds number, the spectrum in the inertial subrange is uniquely determined by ε, and especially it is independent of ν. Using dimensional analysis, it can be deduced that in this range the energy spectrum can be expressed as:

$$E(\kappa) = C_K \varepsilon^{\frac{2}{3}} \kappa^{-\frac{5}{3}} \quad , \tag{2.3}$$

where $C_K = 1.5$ is the universal Kolmogorov constant. This relation is often referred to as the $-5/3$-*power law*. As the anisotropic large scales break down to successively smaller eddies,

they loose the directional information of the mean flow field and the boundary conditions. Consequently, the statistics of the small eddies in the inertial and viscous subrange are isotropic and universal, independent of the boundary conditions. This is the main idea of the *Kolmogorov's hypothesis of local isotropy* and is used as justification of the assumption of isotropy of small-scale motions in many turbulence models.

The length scales that characterize the energy containing scales and the viscous subrange are derived by dimensional analysis.

According to the *first similarity hypothesis of Kolmogorov*, the energy spectrum in the viscous subrange is uniquely determined by ν and ε for sufficiently high Reynolds numbers. Since at the smallest turbulent scales the energy dissipates with the turbulent dissipation rate ε due to the action of the viscosity ν, the length scale of these eddies has to be a function of these two quantities only. By dimensional analysis the Kolmogorov length scale η is found as:

$$\eta = \left(\frac{\nu^3}{\varepsilon}\right)^{\frac{1}{4}} \quad . \tag{2.4}$$

Due to the scale-invariance of ε, the energy dissipation rate can also be used to derive the turbulent length scale l_t, which is associated with the size of the larger integral eddies:

$$l_t = \frac{k^{\frac{3}{2}}}{\varepsilon} \quad . \tag{2.5}$$

Similarly, appropriate time scales can be defined, which are proportional to the turnover time of an eddy of the corresponding length scale. The time scale, which is associated with the eddies of the size of the most energetic eddies, is referred to as the integral time scale τ:

$$\tau = \frac{k}{\varepsilon} \quad . \tag{2.6}$$

The Kolmogorov time scale t_η corresponds to smallest eddies and is defined as:

$$t_\eta = \sqrt{\frac{\nu}{\varepsilon}} \quad . \tag{2.7}$$

Hinze (1987) gave a better understanding of the energy balance of the spectrum deriving a balance equation for $E(\kappa, t)$ for homogenous turbulence with imposed mean velocity gradients to initiate production:

$$E(\kappa, t) = \mathscr{P}_\kappa(\kappa, t) - \frac{\partial}{\partial \kappa}\mathscr{T}_\kappa(\kappa, t) - \mathscr{D}(\kappa, t) \quad . \tag{2.8}$$

$\mathscr{P}_\kappa(\kappa,t)$ represents the production spectrum, which is given by the product of the mean velocity gradients and an anisotropic part of the spectrum tensor (Pope (2000)). $\mathscr{T}_\kappa(\kappa,t)$ is the spectral energy transfer rate, which describes the energy transfer from lower to higher wavenumbers than κ. $\mathscr{D}(\kappa,t)$ denotes the dissipation spectrum, which can be expressed as $\mathscr{D}(\kappa,t) = 2\nu\kappa^2 E(\kappa,t)$.

Fig. 2.2 depicts the distribution over the wavenumber of the different contributions to the balance equation of $E(\kappa,t)$. κ_{EI} and κ_{DI} separate the inertial subrange from the energy containing scales and the viscous subrange, respectively. The sketch is presented for high Reynolds number, where the inertial subrange expands over a large range of length scales and the production and the dissipation spectrum are clearly separated.

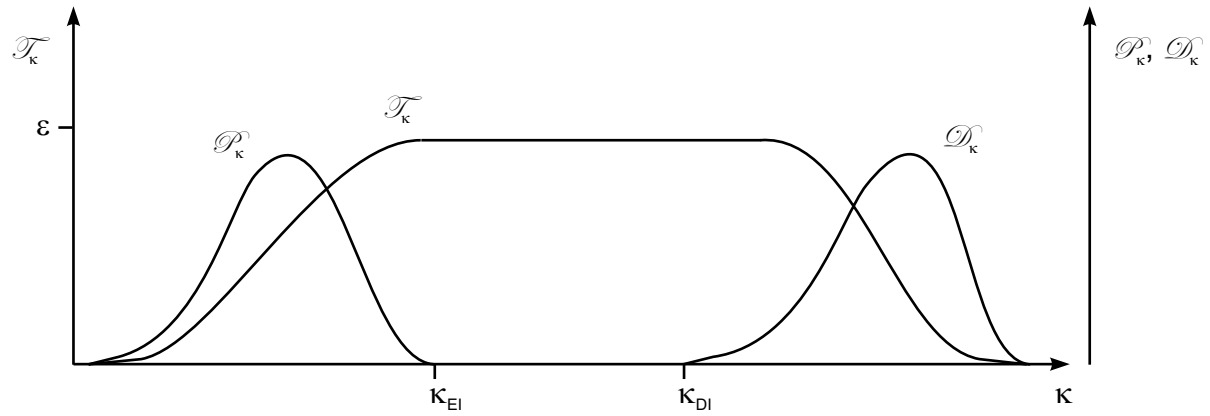

Figure 2.2: Sketch of the different contributions to the balance equation of $E(\kappa,t)$.

It can be observed that $\mathscr{T}_\kappa(\kappa,t)$ vanishes at zero and infinite wavenumber. Thus, $\mathscr{T}_\kappa(\kappa,t)$ makes no contribution to the balance equation of the turbulent kinetic energy and the change of k in time can simply be expressed by the production and the dissipation rate as $dk/dt = \mathscr{P} - \varepsilon$.

2.1.2 Statistical Description of Turbulence

Due to the complexity of a turbulent flow field, it is convenient to investigate turbulence statistically decomposing the instantaneous flow quantities f into the time or ensemble-averaged mean quantity $\overline{f}$ and the fluctuation f' with $f = \overline{f} + f'$. This type of decomposition goes back to Reynolds (1894) and is discussed in section 2.3.1 in further detail.

The energy that is contained in the turbulent fluctuations of the velocity field is the turbulent kinetic energy. It is defined as half of the trace of the Reynolds-stress tensor given in Equation 2.66:

$$k = \frac{1}{2}\overline{u_k' u_k'} \quad . \tag{2.9}$$

Similar to the turbulent kinetic energy k, u_k' is also associated with temporal fluctuations of the complete range of spatial scales. The root-mean-square of the velocity fluctuation u'_{rms} is related to the turbulent kinetic energy by:

$$u'_{rms} = \sqrt{\frac{2}{3}k} \quad . \tag{2.10}$$

It is used to define the turbulent Reynolds number as:

$$Re_t = \frac{u'_{rms}\, l_t}{\nu} \quad . \tag{2.11}$$

Based on the statistics of the velocity field the turbulent dissipation rate is defined as:

$$\varepsilon = \nu \overline{\left(\frac{\partial u'_k}{\partial x_i} \frac{\partial u'_i}{\partial x_k} \right) \frac{\partial u'_k}{\partial x_i}} \quad . \tag{2.12}$$

Since turbulence is a continuous motion, the movement of neighboring points of the velocity field is statistically not independent. The *two-point velocity correlation* relates the velocity fluctuations of two points with the distance $r = |\mathbf{r}|$ and indicates to what degree they influence each other:

$$R_{ij}(\mathbf{r}, \mathbf{x}, t) = \overline{u'_i(\mathbf{x}, t)\, u'_j(\mathbf{x}+\mathbf{r}, t)} \quad . \tag{2.13}$$

For $|\mathbf{r}| = 0$ the Reynolds stress tensor is recovered. The two-point correlation is a simple statistical approach to gain spatial information out of a turbulent flow field. It can be used to identify various length scales such as the integral length scale L^k_{ij}:

$$L^k_{ij}(\mathbf{x}, t) = \frac{1}{R_{ij}(0, \mathbf{x}, t)} \int_0^\infty R_{ij}(r_k, \mathbf{x}, t)\, dr_k \quad . \tag{2.14}$$

If the velocity vectors at the two locations and their distance vector point in the same direction, the length scale will be referred to as the longitudinal integral length scale:

$$L^1_{11}(\mathbf{x}, t) = \frac{1}{\overline{u'^2_1}} \int_0^\infty R_{11}(r_1, \mathbf{x}, t)\, dr_1 \quad . \tag{2.15}$$

Similar to l_t, L^1_{11} is associated with the large energy containing eddies and can be understood as a measure of simultaneously moving fluid particles at an instance of time. Using a von Kármán-Pao type model spectrum, Pope (2000) theoretically showed that for high Reynolds numbers the two length scales are proportional:

$$L^1_{11} \approx 0.43\, l_t \quad . \tag{2.16}$$

Using the two-point velocity correlation, the longitudinal Taylor micro length scale can be introduced:

$$l_\lambda = \left(\frac{\overline{u'^2_1}}{\partial^2 R_{11}/\partial r_1^2} \right)^{1/2} \quad . \tag{2.17}$$

It is always smaller than the integral length scale ($l_\lambda < L^1_{11}$) and their relation is only determined by the Reynolds number. **Fig. 2.3** shows the geometric interpretation of the length scales.

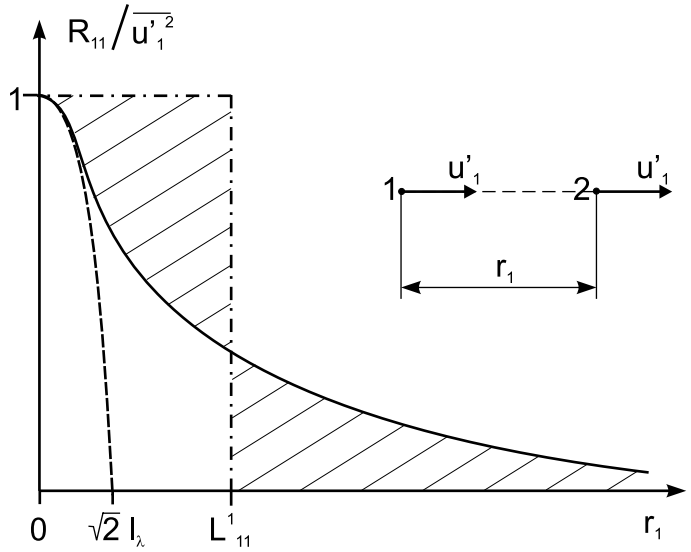

Figure 2.3: Geometric interpretation of the longitudinal integral and Taylor length scale (Rotta (1972)).

For homogeneous and isotropic turbulence the relations can be simplified. The two-point correlation R_{ij} is independent of the location $\mathbf{x}$ and the direction and depends only on the distance r. Thus, it is $\overline{u'^2_1} = \overline{u'^2_2} = \overline{u'^2_3} = \sqrt{\overline{u'_i u'_i}/3} = u'^2_{rms}$. Due to isotropy R_{ij} can be expressed in terms of two scalar functions $f(r,t)$ and $g(r,t)$:

$$R_{ij}(\mathbf{r},t) = u'^2_{rms} \left(g(r,t)\delta_{ij} + [f(r,t) - g(r,t)] \frac{r_i r_j}{r^2} \right) \quad . \tag{2.18}$$

For $\mathbf{r} = \mathbf{e}_1 r$ equation 2.18 simplifies to:

$$\mathrm{f}(r,t) = \frac{R_{11}(r_1,t)}{u'^2_{rms}} \quad , \tag{2.19}$$

$$\mathrm{g}(r,t) = \frac{R_{22}(r_1,t)}{u'^2_{rms}} \quad , \tag{2.20}$$

$$R_{33} = R_{22}, \quad R_{ij} = 0 \quad for \quad i \neq j \quad .$$

The scalar functions f and g can be identified as the longitudinal and transverse auto-correlation, respectively. It can be shown that due to the continuity equation given in Equation 2.35 the two functions can be related. Consequently, for isotropic turbulence the two-point correlation R_{ij} only depends on a single scalar function f or g:

$$\mathrm{g}(r,t) = \mathrm{f}(r,t) + \frac{1}{2} r \frac{\partial}{\partial r} \mathrm{f}(r,t) \quad . \tag{2.21}$$

The longitudinal integral length scale can be expressed then as follows:

$$L_{11}^{1}(t) = \int_0^\infty \mathrm{f}(r,t)\, dr \quad . \tag{2.22}$$

Using the transverse auto-correlation g, the transversal integral length scale reads:

$$L_{22}^{1}(t) = \int_0^\infty \mathrm{g}(r,t)\, dr \quad . \tag{2.23}$$

For homogeneous isotropic turbulence the integral length scales are related as follows:

$$L_{11}^{1} = L_{22}^{2} = L_{33}^{3} \quad \textit{and} \tag{2.24}$$

$$L_{ii}^{j} = \frac{L_{ii}^{i}}{2} \quad \textit{for} \quad i \neq j \quad . \tag{2.25}$$

Similar to the two-point velocity correlation R_{ij} the *second order velocity structure function* D_{ij} is sufficiently determined by one scalar function D_{LL}, which is referred to as the longitudinal structure function. D_{ij} is defined as:

$$\mathsf{D}_{ij}(\mathbf{r},\mathbf{x},t) = \overline{\left(u_i'(\mathbf{x}+\mathbf{r},t) - u_i'(\mathbf{x},t)\right)\left(u_j'(\mathbf{x}+\mathbf{r},t) - u_j'(\mathbf{x},t)\right)} \quad . \tag{2.26}$$

The longitudinal structure function D_{LL} is related to the longitudinal auto-correlation f(r). According the second similarity hypothesis, D_{LL} is sufficiently determined by ε and r in the inertial subrange:

$$\mathsf{D}_{LL}(r,t) = 2u_{rms}'^{2}\left(1 - \mathrm{f}(r)\right) = C_2 (\varepsilon r)^{2/3} \quad . \tag{2.27}$$

where C_2 is a universal constant. This formulation corresponds to the Kolmogorov's $-5/3$-power law for the energy spectrum given in equation 2.3.

The two velocity correlations can be used to define various important length scales and to apply the Kolmogorov hypothesis. This gives the opportunity to compare the relations deduced directly with experimental data and to evaluate theories and hypotheses in turbulence research. For a more detailed description the reader is referred to Rotta (1972) or Pope (2000).